Seasonal prediction of the intraseasonal variability of the West African monsoon precipitation

LUIS RICARDO LAGE RODRIGUES[1], JAVIER GARCIA-SERRANO[1,2] & FRANCISCO DOBLAS-REYES[1,3]

[1] Institut Català de Ciències del Clima (IC3), Barcelona, Spain
[2] Laboratoire d'Océanographie et du Climat, Université Pierre et Marie Curie (UPMC), Paris, France
[3] Institució Catalana de Recerca i Estudis Avançats (ICREA), Barcelona, Spain
luis.rodrigues@ic3.cat

Received: 08/04/2013
Accepted: 17/07/2013

Abstract
In this paper we review the main modes of variability associated with the West African monsoon (WAM) rainfall as predicted by three operational forecast systems: the ECMWF System 4 (S4), NCEP CFSv2 (CFSv2), and the Météo-France System 3 (MF3). A new methodology to assess the interannual variations of the WAM rainfall is considered, where monthly rainfall is averaged zonally over 10ºW-10ºE before estimating the two leading modes of WAM rainfall variability. It is found that S4 is skilful when predicting the two leading modes of WAM rainfall variability, MF3 is skilful when predicting the Guinean regime, and CFSv2 has no skill when predicting the Guinean regime and low correlation when predicting the Sahelian regime.
Key words: West African monsoon, seasonal prediction, operational forecast systems

Predicción estacional de la variabilidad intra-estacional de la precipitación del Monzón de África Occidental

Resumen
En este trabajo revisamos los principales modos de variabilidad asociados con la precipitación del Monzón de África Occidental (MAO) tal como lo predicen tres sistemas operacionales de predicción: el System 4 (S4) de ECMWF, NCEP CFSv2 (CFSv2), y el Météo-France System 3 (MF3). Se emplea una nueva metodología para evaluar las variaciones interanuales de la precipitación del MAO, en el que la precipitación mensual se promedia zonalmente entre 10ºW-10ºE antes de estimar los dos modos de dominantes de variabilidad de la precipitación de MAO. Se obtiene que S4 muestra habilidad para predecir los dos primeros modos de variabilidad de la precipitación de MAO, MF3 muestra habilidad para predecir el régimen Guineano, y CFSv2 no muestra habilidad para predecir el régimen Guineano y muestra correlaciones bajas para predecir el régimen del Sahel.
Palabras clave: Monzón de África Occidental, predicción estacional, sistemas de predicción operacionales

Física de la Tierra
Vol. 25 (2013) 73-87
ISSN: 0214-4557
http://dx.doi.org/10.5209/rev_FITE.2013.v25.43436

Normalized reference
Rodrigues, L. R. L, García-Serrano, J., Doblas-Reyes, F. (2013) Seasonal prediction of the intraseasonal variability of the West African monsoon precipitation. *Física de la Tierra*, Vol. 25, 83-97.

1. Introduction

Associated with the apparent motion of the sun, the Intertropical Convergence Zone (ITCZ) experiences a latitudinal shift along the year which plays a fundamental role on determining the West African monsoon (WAM) rainfall variability (Motha et al., 1980). The WAM rainfall variability spans a wide range of timescales, from intraseasonal (e.g. Sultan et al., 2003) to interdecadal (e.g. Nicholson, 1993), and is influenced by both local and remote oceanic forcings and associated changes in the atmospheric circulation (Folland et al., 1986; Fontaine et al., 1995; Fontaine and Janicot, 1996; Fontaine et al., 1998; Janicot et al., 1998; Janicot et al., 2001).

Motha et al. (1980) analyzed long-term rainfall data in Nigeria and found two distinct rainfall patterns. In one of them, rainfall anomalies of opposite signs are observed in the Sahelian and Guinean regions. They suggested that this was associated with the latitudinal migration of the ITCZ such as that above (below) normal rainfall in the Sahelian (Guinean) region is observed when the ITCZ is placed further north of its climatological position. Rainfall pattern with below (above) normal rainfall in the Sahelian (Guinean) region takes place when the ITCZ does not penetrate into the Sahelian region with its normal intensity. In the second pattern, rainfall anomalies with the same sign are experienced throughout the WAM region. These precipitation modes show, likewise, low-frequency modulation of their spatial extent (see Rodríguez-Fonseca et al. 2011 for a review).

Other studies found similar patterns of summer WAM rainfall variability (Fontaine et al., 1995; Fontaine and Janicot, 1996; Janicot et al., 1998). They examined the connection of these patterns with sea surface temperature (SST) anomalies (Fontaine and Janicot, 1996; Janicot et al., 1998) and monthly tropospheric wind change (Fontaine et al., 1995). The two leading modes of WAM rainfall variability, extracted by using principal component analysis (PCA), correspond to the rainfall variability along the Sahelian and Guinean regions (Giannini et al., 2003, Giannini et al., 2005; Philippon et al., 2010; Tippet and Giannini, 2006). While the Guinean rainfall regime is mostly explained by interannual variations, the variability in the semi-arid Sahelian region occurs mostly on decadal time scales although interannual variations also play a role in this region, specially linked to the El Niño-Southern Oscillation (ENSO) (Giannini et al., 2003, Giannini et al., 2005; Fontaine et al., 1998; Janicot et al.,

2001; Tippet and Giannini, 2006). It is worth noting that the internal variability may be important for the WAM rainfall variability, even at decadal time scale.

Atmospheric general circulation models (AGCMs) forced with observed SSTs are able to simulate successfully these two rainfall regimes (Giannini et al. 2003, Giannini et al., 2005; Tippet and Giannini, 2006). However, Goddard and Mason (2002) compared the ensemble-mean anomaly correlation simulated and predicted by an AGCM using persisted SST anomalies and found that errors in the predicted SST could lead to a significant degradation of the predictive skill. They showed that WAM rainfall during the July-August season is one of the most severe examples of this loss of prediction skill. In addition, predictive skill can be negatively affected if the model used to take advantage of SST information does not properly describe the mechanism responsible for the WAM rainfall (Krishna Kumar et al., 2005).

Philippon et al. (2010) found that the Guinean rainfall regime could be accurately predicted by the ENSEMBLES Stream 1 coupled GCMs (hereafter referred to as forecast system), but not the Sahelian regime.

In this study, we assess the ability of three operational forecast systems to predict the two leading modes of WAM rainfall variability. The forecast systems are the ECMWF seasonal forecast system 4 (S4; Molteni et al., 2011), the National Centers for Environmental Prediction (NCEP) climate forecasting system version 2 (CFSv2; Saha et al., 2011) and the Météo-France System 3 (MF3; Alessandri et al., 2011). A new methodology to assess the interannual variations of the WAM rainfall is considered, where monthly rainfall is averaged zonally over 10ºW-10ºE before estimating the two leading modes of WAM rainfall variability. The aim is to assess the ability of these forecast systems to predict the evolution of the meridional displacement of the rainfall and its intraseasonal evolution.

In section 2, the observations and the forecast systems are described. Section 3 describes how the two leading modes of WAM rainfall variability are estimated. Section 4 shows the results and Section 5 the conclusions.

2. Data

Two observational precipitation datasets have been used in this study: the version 2.2 of the Global Precipitation Climatology Project (GPCP) monthly satellite-gauge combined (Huffman and Bolvin, 2013) and the version 4.0 of the Global Precipitation Climatology Center (GPCC) monthly gridded gauge-analysis derived from quality controlled station data (Schneider et al., 2011). The GPCP dataset has a 2.5º resolution and covers both land and ocean. The period of the GPCP data is from 1979 onwards. On the other hand, the 1º resolution GPCC dataset is available only over land and the period from 1901 onwards. The GPCP dataset is used for the validation of the forecast systems while both datasets are used to assess the observation uncertainty.

The atmospheric component of S4 is the cycle 36r4 of the ECMWF Integrated Forecast System (IFS) (Kim et al., 2012; Molteni et al., 2011). It has a horizontal resolution of about 80 km and 91 vertical levels, extending up to about 0.01 hPa. The ocean component of S4, the Nucleus for European Modelling of the Ocean (NEMO) version 3.0, has a horizontal resolution of about 1º with equatorial refinement and 42 vertical levels, 18 of which are in the upper 200 m. S4's hindcasts have 15 ensemble members, all starting in burst mode on the first day of every month at 0 UTC. The simulations are seven-month long and cover the period 1981-2010.

CFSv2 uses the NCEP Global Forecast System (GFS), with horizontal resolution of about 100 km and 64 vertical levels, as its atmospheric component (Kim et al., 2012; Saha et al., 2011; Yuan et al., 2011). Its ocean component is the Geophysical Fluid Dynamics Laboratory Modular Ocean Model version 4 (MOM4) and it has maximum horizontal resolution of 0.25º within 10º of the equator and 0.5º poleward and 40 vertical levels. CFSv2 hindcasts have 24 ensemble members, except November that has 28 members. The hindcasts are initialized in different days and times, being the ones initialized after the day 7 used as the lead time zero ensemble members of the next month. For example, the ensemble members for the target month of February at lead time zero have start dates in January 11th, 16th, 21st, 26th, 31st, and the February 5th (at the synoptic times 00, 06, 12 and 18 UTC) of the same year. The simulations are ten-month long and cover the period 1982-2010.

MF3 uses the Action de Recherche Petite Echelle Grande Echelle (ARPEGE) version 4 as its atmospheric component (Alessandri et al., 2011). It has a horizontal resolution of about 300 km and 91 vertical levels, reaching high into the stratosphere. Its ocean component ORCA, is the global version of the Océan PArallélisé (OPA) model version 8.2, has horizontal resolution of about 2º and 31 vertical levels. MF3´s hindcasts have 11 ensemble members, all starting in burst mode on the first day of every month at 0 UTC. The simulations are seven-month long and cover the period 1981-2010.

3. Methods

The deterministic skill of the three operational forecast systems described above is assessed at each grid-point over the WAM region (22ºW - 22ºE; 0º - 22ºN) to verify whether these systems are able to simulate the WAM rainfall. The correlation coefficient is used to assess the degree of linear correspondence between the predicted and observed July, August and September (JAS) rainfall. A simple multi-model ensemble mean (SMM), where all dynamical forecast systems are put together with equal weighting, is used as a benchmark.

Monthly rainfall is averaged zonally over 10ºW-10ºE to assess both the role of the latitudinal migration and the intraseasonal distribution of rainfall on the WAM rainy season. This longitudinal range is chosen to represent the core of the WAM

rainfall. The analysis is performed across the meridional range between the Equator and 20ºN and the period between June and October. The southernmost limit is intended to capture the inland penetration of monsoonal rainfall over the Guinean region, while the northernmost limit tries to capture the Sahelian rainfall, which usually reaches 18ºN. The period chosen is from June to October where June and October are one month prior to and one month after the JAS target season. The upper limit of the forecast time is seven months (the longest forecast time of both S4 and MF3) and allows the analysis for three start dates: June (lead 0), May (lead 1) and April (lead 2).

The GPCP and GPCC datasets for the period 1982-2010 and 1951-2010, respectively, are used to assess the uncertainties associated with the observations. The year 1982 is the first year available for the seasonal hindcasts, while the year 1951 is the year from which a large number of stations are used in the GPCC data, and therefore, makes it a more trustworthy period for this dataset (Schneider et al., 2011). The GPCP dataset is also used with a mask over the ocean to compare with the GPCC over the common period 1982-2010. Hence, the climatologies of the observed zonally averaged rainfall are computed using the four datasets: GPCP 1982-2010, GPCP land-only 1982-2010, GPCC 1951-2010 and GPCC 1982-2010. The climatologies and the systematic errors of the predicted zonally averaged rainfall are computed against the GPCP for the period 1982-2010 and for the three start dates, April, May and June.

Principal component analysis (PCA; Wilks, 2006) is performed on the observed and predicted zonally averaged rainfall to estimate the leading modes of WAM rainfall variability. The anomalies, estimated for both observations and forecast systems prior to applying the PCA, were computed using three-years out cross-validation mode to avoid artificial skill in the forecast quality assessment. The leading modes of the WAM rainfall variability are described as a set of spatial patterns (empirical orthogonal functions, EOFs) and associated standardized time series (principal components, PCs). The PCA is performed on the observations and on each forecast system and lead time separately to take into account the individual system's systematic errors (Doblas-Reyes et al., 2003; Philippon et al., 2010). The correlation coefficient between the predicted ensemble mean and observed PCs for each forecast system and lead time is computed to assess to what extent the current operational forecast systems capture the two leading modes of WAM variability.

4. Results

Figure 1 shows the correlation between the predicted ensemble mean and the observed JAS rainfall at each grid point over the WAM region for the period 1982-2010. The correlation is computed for the three forecast systems and their combination. S4 has positive correlation in almost all grid points at the three lead times analyzed. Even though the SMM also has positive correlation in most cases,

its correlation is lower than S4´s more often than not. On the other hand, CFSv2 has low, and in several instances, negative correlation values. Most of the positive correlation values in this forecast system appear north of 10ºN, over the continental Sahel. MF3 also has lower skill when compared to S4, but contrary to CFSv2, most of the positive correlation appear south of 10ºN, in the Guinean region over the longitudinal range 20ºW-10ºE. S4 has the highest overall correlation at all lead times, followed by the SMM, MF3, and CFSv2. Also the correlation does not change significantly with lead time. Surprisingly S4 has very high correlation at the grid-point level when compared to the other single systems and the SMM. This is surprising because the previous ECMWF forecast systems have similar skill to its counterparts (Batté and Déqué, 2011). Molteni et al. (2011) found a clear improvement in the simulation and prediction of ocean/atmosphere variability in the tropical Atlantic and adjacent regions, specifying the WAM region. They highlight that some of the improvements S4 has achieved when compared to its predecessor are due to higher horizontal and vertical resolution, a more accurate initialization of the land-surface variables, improved physical parameterization, among others.

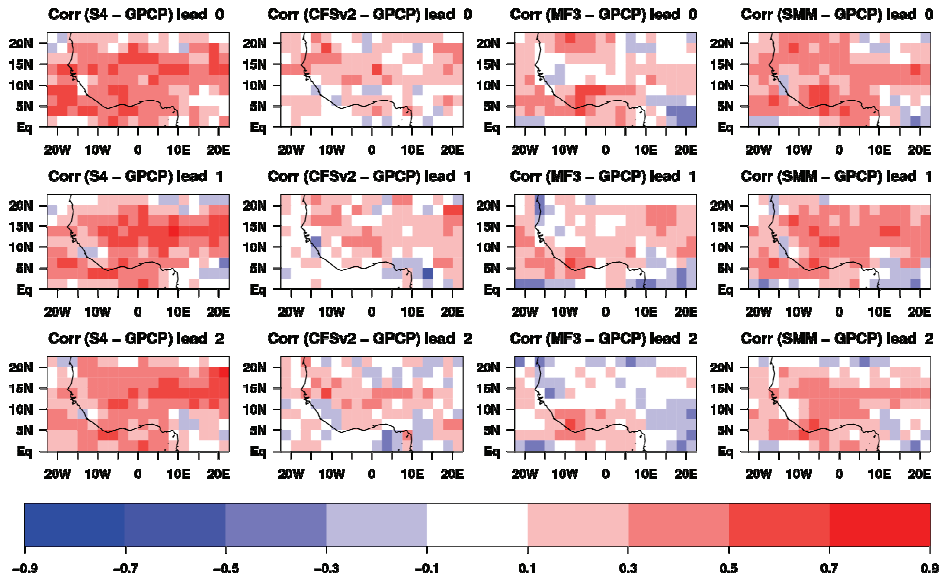

Fig. 1. Correlation coefficient between the predicted ensemble mean and observed summer (JAS) rainfall at each grid-point over the WAM region for the period 1982-2010. The GPCP was used as the reference data. Lead times increase with row from top to bottom. Each column is for one forecast system: from left to right, S4, CFSv2, MF3 and the SMM.

In order to understand the causes of the ensemble-mean skill shown above, a discussion of the observed and predicted mean climate and its variability is discussed below. The climatologies of the zonally averaged monthly rainfall have similar pattern in both observational datasets (Figure 2). They show a northward migration of the rainfall that reaches its northernmost position at 18ºN in JAS, moving southward later on. The three forecast systems successfully simulate the meridional shift of the rainfall for the three lead times analyzed (Figure 2 illustrates for lead time 1). However, they all fail to simulate the position of the rainfall maxima and have substantial biases, suggesting that these systems do not reproduce well the physical processes associated with the WAM rainfall. The bias pattern suggests that the forecast systems simulate the ITCZ rainfall band in the wrong position, that is, the simulated ITCZ does not penetrate as far north as in the observations creating a dipole-like bias pattern (i.e. excessive precipitation at lower latitudes and deficit at higher latitudes).

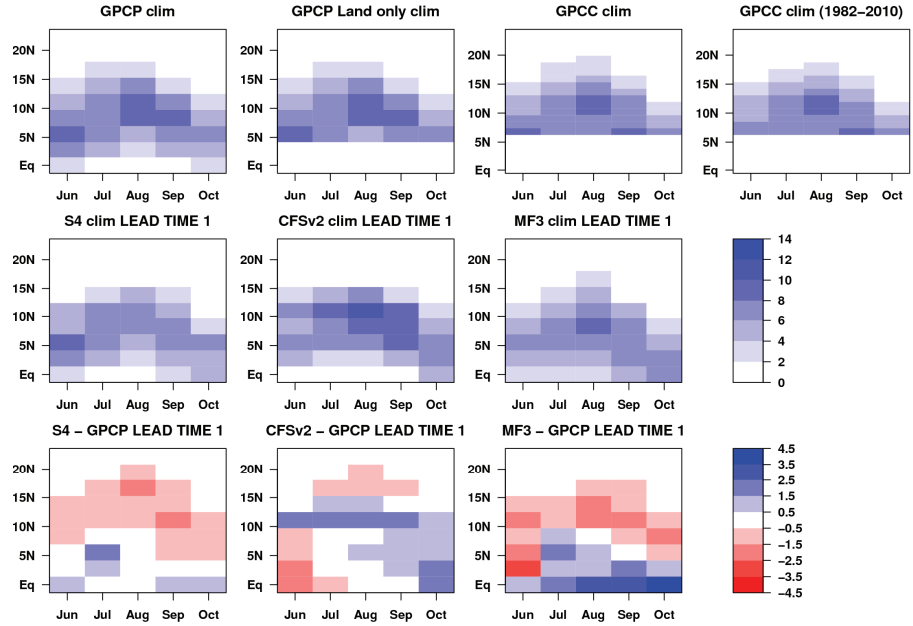

Fig. 2. Monthly rainfall averaged over 10ºW-10ºE and for the period between June and October. Climatologies of the two analyzed observational datasets and the three dynamical forecast systems for the start date of May (are shown in the first two rows). GPCP and GPCC climatologies were computed using the period 1982-2010 and 1951-2010, respectively. For comparison the GPCP climatology was also computed masking the ocean and the GPCC using only the common period 1982-2010. The systematic error of the dynamical forecast systems was computed against the GPCP dataset. All dynamical forecast systems were interpolated into the GPCP resolution before estimating the systematic error. Units are in mm/day.

The two leading modes of WAM rainfall variability are shown in Figure 3. The first EOF (EOF1) in the GPCP data shows a dipole pattern with positive values south of 10ºN, in the Guinean region, and negative values above it. The second EOF (EOF2) shows only positive values in the Hovmöller diagram and a maximum north of 10ºN, in the Sahelian region. The variance associated with these two EOFs is 28% and 22%, respectively. This is in agreement with the WAM patterns described in the literature using different methodologies (Fontaine et al., 1995; Fontaine and Janicot, 1996; Janicot et al., 1998; Motha et al., 1980). The GPCP land only and the GPCC datasets have a reverse order of the leading modes. This reversal is probably due to the variance maximization of inland precipitation, where the latitudinal migration from the ocean of the Guinean rainfall early in the season is not considered. However, the variance explained by these two EOFs varies according to the data used, being 31% (EOF1) and 23% (EOF2) in the GPCP land only, 26% and 20% in the GPCC, and 30% and 17% in the GPCC for the period 1982-2010.

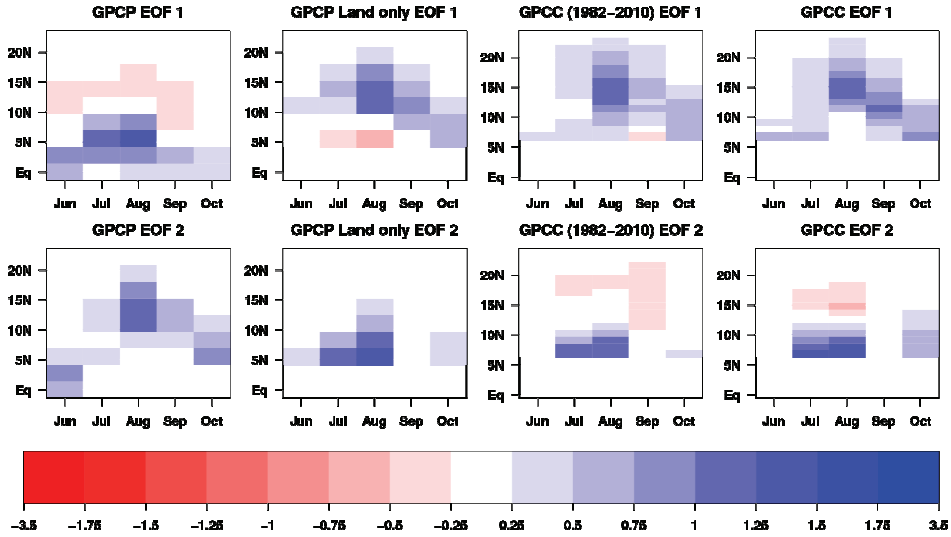

Fig. 3. First two EOFs of the observed Hovmoler diagram by GPCP and GPCC datasets shown in the first row of Figure 2.

To illustrate that the Guinean regime is captured in the EOF1 (EOF2) when the dataset have observations over both land and ocean (land only) and vice-versa for the Sahelian regime, the PCs associated with these EOFs are displayed in Figure 4. The first PC (PC1) of the GPCP is highly correlated with the second PC (PC2) of the GPCP land only and GPCC and vice versa. The GPCC PCs show that the Guinean regime is characterized mainly by interannual variability while the

Sahelian regime is associated with substantial interdecadal variations as described in previous studies. It is observed that the interannual variability of the Guinean regime was stronger before the 70s than after that date, a feature not found, for example, in Giannini et al. (2003) and Giannini et al. (2005) although they used different methodology to define the WAM rainfall regimes.

The three operational forecast systems, which predict rainfall over both land and ocean, reproduce well the EOFs associated with the Sahelian and Guinean regimes as they locate the positive values south of 10ºN in the EOF1 and north of it in the EOF2 (Figure 5 illustrates for lead time 1). However, they are clearly biased. For instance, all the forecast systems locate the negative values south of 10ºN in the EOF2 in August. MF3 does not capture the negative values north of 10ºN in the EOF1 but add negative values south of 10ºN in June in the EOF2. S4 and CFSv2 present similar patterns at lead time 0 and 2 months as the ones shown in Figure 5 while MF3 fail to capture the rainfall north of 10ºN in the Sahelian regime at these leads (not shown). S4 usually overestimates the variance associated with EOF1 (34% for lead time 1) and underestimates the variance associated with EOF2 (13% for lead time 1). In addition, S4 increases (decreases) the variance associated with the EOF1 (EOF2) with lead time. CFSv2 (19% and 10% for lead time 1) and MF3 (19% and 11% for lead time 1) underestimate the variance associated with both modes at all lead times.

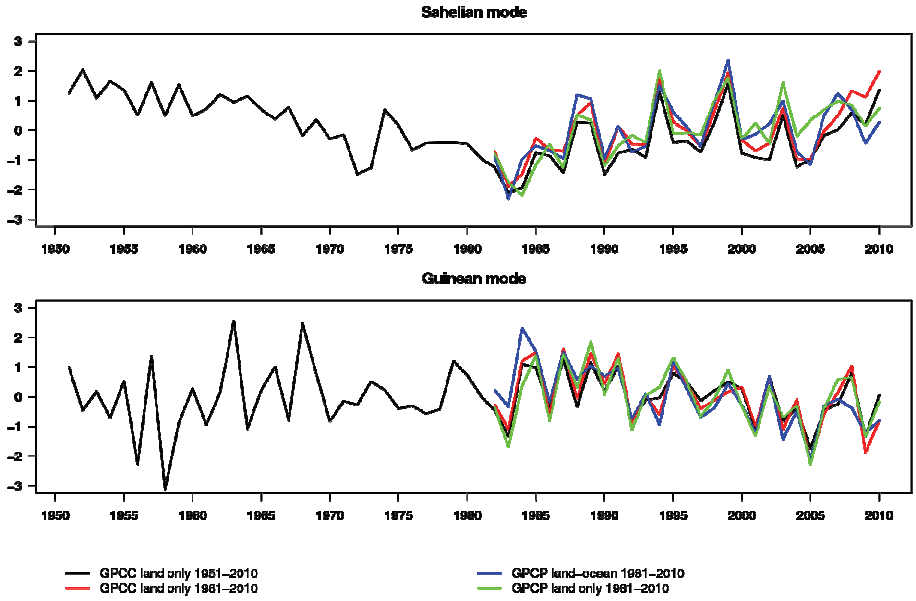

Fig. 4. Principal components associated with the EOFs shown in Figure 3.

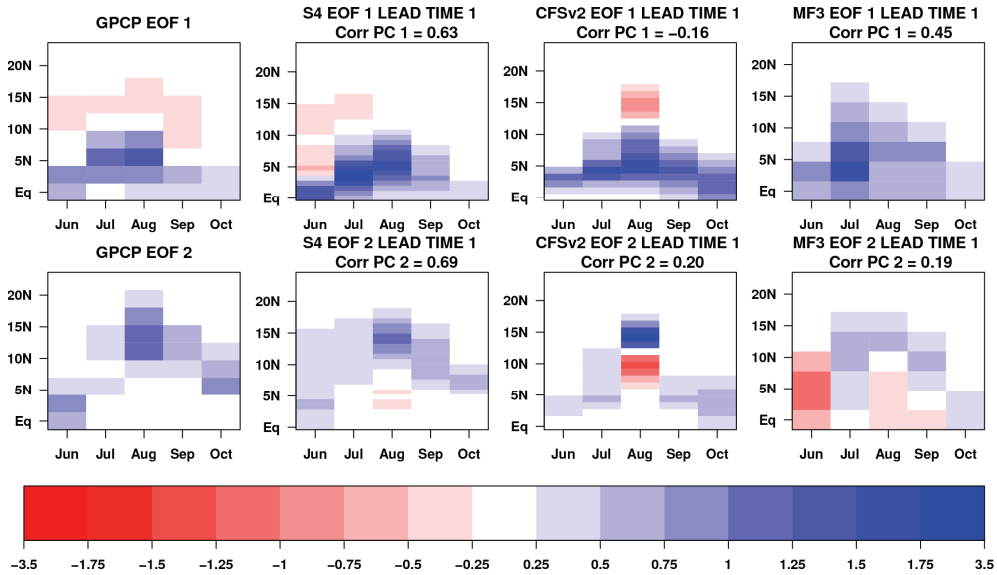

Fig. 5. Leading two EOFs of the GPCP, S4, CFSv2 and MF3 precipitation predictions described in Figure 2. Predictions are for lead time 1 (start date in May). EOF1 is displayed in the upper panel and EOF2 in the lower panel.

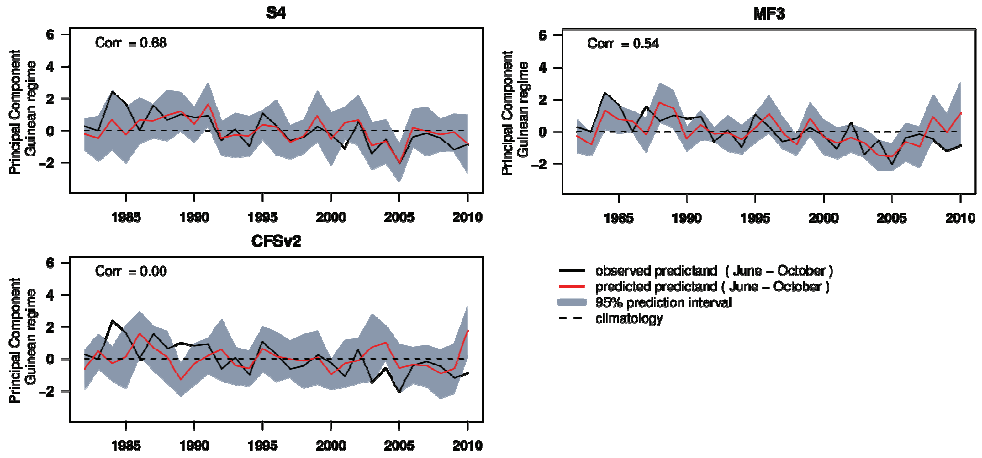

Fig. 6. Leading principal component (Guinean regime) of the S4, CFSv2 and MF3 precipitation predictions described in Figure 2. Predictions are for lead time 0 (start date in June). Observed values (black solid line), predicted values (red solid line), 95 % predicted interval (grey area) and the climatology value (black dashed line). The values displayed are anomalies. The zero line shows the approximate location of the climatology. The correlation coefficient is displayed in each panel.

Figure 6 illustrates the PCs for the Guinean regime predicted by the three operational forecast systems: S4, CFSv2 and MF3. Predictions are for lead time 0 (i.e. predictions starting in June). The correlation coefficient between the predicted ensemble-mean (red solid line) for each forecast system and the observed GPCP PC (black solid line) is displayed. The climatology value (black dashed line) is shown for reference. S4 and MF3 reproduce well the interannual variability and are well correlated with the observed GPCP PC for this lead time. On the other hand, CFSv2 although presents interannual variability, it does not correlate with the observed PC.

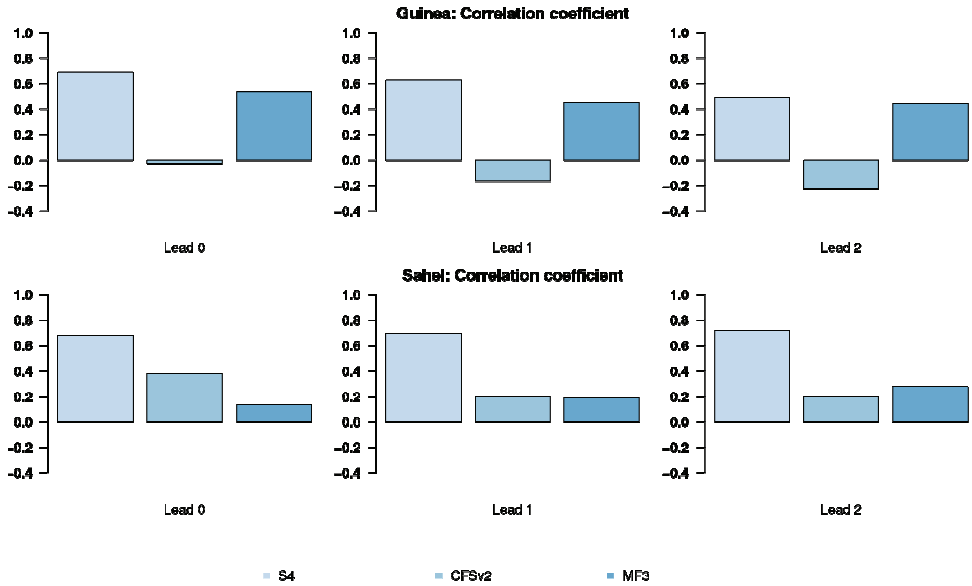

Fig. 7. Correlation coefficient between the observed and predicted ensemble mean PCs for the period 1982-2010. The correlation was computed for the Sahelian (upper panel) and Guinean (lower panel) rainfall regimes and for lead times one, two and three. The bars in each histogram represent the forecast systems: from left to right, S4, CFSv2 and MF3.

The correlation coefficient between the observed and predicted ensemble mean PCs quantifies the degree of linear association between the leading modes estimated by the GPCP and each forecast system (Figure 7). S4 has the highest correlation when predicting both rainfall regimes at all lead times. It is worth noting that S4 is far better than its predecessor when predicting the WAM rainfall regimes (Molteni et al., 2011). The correlation of S4 and MF3 does not decrease with lead time when predicting the Sahelian regime. S4 have correlations above 0.6 in all cases except for the Guinean regime at lead time 2 months and MF3 is only competitive when predicting the Guinean regime with average correlation of

about 0.45. On the other hand, CFSv2 has no skill when predicting the Guinean regime and low correlation when predicting the Sahelian regime (expect for lead time 0). In most cases CFSv2 has the lowest ensemble-mean skill in spite of the fact that it has the largest ensemble size (24 members) compared to 15 members of S4 and 11 members of MF3. This means that other characteristics of the forecasts might be more relevant for the WAM rainfall variability, such as the horizontal resolution (80 km for S4, 100 km for CFSv2, 300 km for MF3), vertical resolution, improved physical parameterizations and ocean analysis, etc. The probabilistic forecast quality of the WAM modes of rainfall variability will be described in a future publication.

5. Conclusions

In this paper we study the main modes of variability associated with the West African Monsoon (WAM) rainfall: the Guinean and Sahelian regimes. The ability of three operational dynamical forecast systems to predict the two leading modes of WAM rainfall variability is assessed. A new methodology to assess the interannual variations of the WAM rainfall is considered, where monthly rainfall is averaged zonally over 10ºW-10ºE before estimating the two leading modes of WAM rainfall variability. The aim is to assess the ability of these forecast systems to predict the evolution of the rainbelt latitudinal displacement. It is found that S4, CFSv2 and MF3 are able to capture the main features associated with the two leading modes of WAM rainfall variability, the Guinean and Sahelian regimes. However, they fail to correctly reproduce the variance associated with these two modes. While S4 usually overestimates the variance associated with the EOF1 (34% for lead time 1, compared to 28% of GPCP) and underestimates the variance associated with the EOF2 (13% for lead time 1, compared to 22% of GPCP), CFSv2 (19% and 10% for lead time 1) and MF3 (19% and 11% for lead time 1) underestimate the variance associated with both modes. The correlation between the predicted and observed PC shows that S4 is skilful when predicting the two leading modes of WAM rainfall variability, MF3 is skilful when predicting the Guinean regime, and CFSv2 has no skill when predicting the Guinean regime and low correlation when predicting the Sahelian regime. Therefore, this study shows that even though some of the currently available operational forecast systems still have difficulties of forecasting the WAM modes of rainfall variability S4 is skilful when predicting the ensemble mean PC associated with the Sahelian and Guinean regimes. It is worth noting that S4's predecessor (ECMWF System 3) failed to predict the WAM rainfall regimes (Molteni et al., 2011). Improved horizontal and vertical resolution, a more accurate initialization of the land-surface variables, improved physical parameterization and ocean analysis might be some of the reasons to explain why

S4 performs far better than the CFSv2 and MF3 when predicting the WAM rainfall regime. The use of other combination methods, an alternative simple statistical model to predict the WAM rainfall regime, the forecast quality of probability predictions and S4's performance for longer lead times will be addressed in a future study.

6. Acknowledgements

This study was supported by the Spanish MINECO-funded RUCSS project (CGL2010-20657), the European Union's FP7-funded QWeCI (ENV-2009-1-243964) and SPECS (ENV- 3038378), and the Catalan Government.

7. References

ALESSANDRI, A., A. BORRELLI, A. NAVARRA, A. ARRIBAS, M. DÉQUÉ, P. ROGEL & A. WEISHEIMER (2011). Evaluation of Probabilistic Quality and Value of the ENSEMBLES Multimodel Seasonal Forecasts: Comparison with DEMETER. *Mon. Wea. Rev*., 139, 581-607.

BATTÉ, L. & M. DÉQUÉ (2011). Seasonal predictions of precipitation over Africa using coupled ocean-atmosphere general circulation models: skill of the ENSEMBLES project multimodel ensemble forecasts. *Tellus A*, 63, 283-299.

DOBLAS-REYES, F.J., V. PAVAN & D.B. STEPHENSON (2003). The skill of multi-model seasonal forecasts of the wintertime North Atlantic Oscillation. *Clim. Dyn*., 21, 501-514.

FOLLAND, C.K., T.N. PALMER & D.E. PARHER (1986). Sahel rainfall and worldwide sea surface temperature. *Nature*, 320, 602-607.

FONTAINE, B., S. JANICOT & V. MORON (1995). Rainfall anomaly patterns and wind field signals over West Africa in August (1958-1989). *J. Clim*., 8, 1503-1510.

FONTAINE, B. & S. JANICOT (1996). Near-global sea surface temperature variability associated with West African rainfall anomaly types. *J. Clim*., 9, 2935-2940.

FONTAINE, B., S. TRZASKA & S. JANICOT (1998). Evolution of the relationship between near global and Atlantic SST modes and the rainy season in West Africa: statistical analyses and sensitivity experiments. *Clim. Dyn*., 14, 353-368.

GIANNINI, A., R. SARAVANAN & P. CHANG (2003). Oceanic forcing of Sahel rainfall on interannual to interdecadal timescales. *Science*, 302, 1027-1030.

GIANNINI, A., R. SARAVANAN & P. CHANG (2005). Dynamics of the boreal summer African monsoon in the NSIPP1 atmospheric model. *Clim. Dyn*., 25, 517-535.

GODDARD, L. & S. J. MASON (2002). Sensitivity of seasonal climate forecasts to persisted SST anomalies. *Clim. Dyn*., 19, 619-632.

JANICOT, S., A. HARZALLAH, B. FONTAINE & V. MORON (1998). West African monsoon dynamics and eastern equatorial Atlantic and Pacific SST anomalies. *J. Clim*., 11, 1874-1882.

JANICOT, S., S. TRZASKA & I. POCCARD (2001). Summer Sahel-ENSO teleconnection and decadal time scale SST variations. *Clim. Dyn*., 18, 303-320.

KIM, H.M., P.J. WEBSTER & J.A. CURRY (2012). Seasonal prediction skill of ECMWF System 4 and NCEP CFSv2 retrospective forecast for the Northern Hemisphere Winter. *Clim Dyn*. doi: 10.1007/s00382-012-1364-1366.

HUFFMAN, G.J. & D.T. BOLVIN (2013). GPCP Version 2.2 Combined Precipitation Data Set Documentation, Internet Publication, 1-46. Available at: http://www1.ncdc.noaa.gov/pub/data/gpcp/gpcp-v2.2/doc/V2.2_doc.pdf. Accessed: 16 November 2012.

KRISHNA KUMAR, K., M. HOERLING & B. RAJAGOPALAN (2005). Advancing dynamical prediction of Indian monsoon rainfall. *Geophys. Res. Lett*., 32, L08704, doi:10.1029/2004GL021979.

MOLTENI, F., T. STOCKDALE, M. BALMASEDA, G. BALSAMO, R. BUIZZA, L. FERRANTI, L. MAGNUSSON, K. MOGENSEN, T. PALMER & F. VITART (2011). The new ECMWF seasonal forecast system (System 4). ECMWF Technical Memorandum 656, pp. 51. http://www.ecmwf.int/publications/library/do/references/list/14. Accessed 20 December 2012

MOTHA, R.P., S.K. LEDUC, L.T. STEYAERT, C.M. SAKAMOTO & N.D. STROMMEN (1980). Precipitation Patterns in West Africa. *Mon. Wea. Rev*., 108, 1567-1578.

NICHOLSON, S.E. (1993). An overview of African rainfall fluctuations of the last decade. *J. Clim*., 6, 1463-1466.

PHILIPPON, N., F.J. DOBLAS-REYES & P.M. RUTI (2010). Skill, reproducibility and potential predictability of the West African monsoon in coupled GCMs. *Clim Dyn*, 35, 53-74.

RODRÍGUEZ-FONSECA, B., S. JANICOT, E. MOHINO, T. LOSADA, J. BADER, C. CAMINADE, F. CHAUVIN, B. FONTAINE, J. GARCÍA-SERRANO, S. GERVOIS, M. JOLY, I. POLO, P. RUTI, P. ROUCOU & A. VOLDOIRE (2011). Interannual and decadal SST-forced responses of the West African Monsoon. *Atmos. Sci. Lett*., 12, 67-74.

SAHA., S., S. MOORTHI, X. WU, J. WANG, S. NADIGA, P. TRIPP, H.L. PAN, D. BEHRINGER, Y.T. HOU, H. CHUANG, M. IREDELL, M. EK, J. MENG, R. YANG (2011). The NCEP Climate Forecast System version 2. J Clim submitted

SCHNEIDER, U., A. BECKER, A. MEYER-CHRISTOFFER, M. ZIESE & B. RUDOLF (2011). Global Precipitation Analysis Products of the GPCC. Global Precipitation Climatology Centre (GPCC), DWD, Internet Publikation, 1-13.

Available at: http://www.dwd.de/bvbw/generator/DWDWWW/Content/Oeffentlichkeit/KU/KU4/KU42/en/Reports__Publications/GPCC__intro__products__2011,templateId=raw,property=publicationFile.pdf/GPCC_intro_products_2011.pdf. Accessed: 16 November 2012.

SULTAN, B., S. JANICOT & A. DIEDHIOU (2003). The West African monsoon dynamics. Part I: documentation of intraseasonal variability. *J. Clim*., 16, 3389-3406.

TIPPET, M.K. & A. GIANNINI (2006). Potentially predictable components of African summer rainfall in an SST-forced GCM simulation. *J. Clim*., 19, 3133-3144.

WILKS, D. (2006). *Statistical methods in the atmospheric sciences*. Second edition, International Geophysics Series, Vol. 59, Academic Press, 627 pp.

YUAN, X., E.F. WOOD, L. LUO & M. PAN (2011). A first look at Climate Forecast System version 2 (CFSv2) for hydrological seasonal prediction. *Geophys Res Lett*. doi:10.1029/ 2011GL047792